

Fatty acid-indole fluorescent derivatives as probes to measure the polarity of interfaces containing gangliosides

Luis A. Bagatolli^a, Guillermo G. Montich^a, Mario Ravera^b, Jorge D. Perez^b,
Gerardo D. Fidelio^{*a}

^a*Departamento de Química Biológica-CIQUIBIC, Facultad de Ciencias Químicas, Universidad Nacional de Córdoba, Ciudad Universitaria, Casilla de Correo 61, 5016-Córdoba, Argentina*

^b*Departamento de Química Orgánica-INFIQC, Facultad de Ciencias Químicas, Universidad Nacional de Córdoba, Córdoba, Argentina*

Received 19 June 1995; revision received 21 August 1995; accepted 25 August 1995

Abstract

The fluorescence emission properties of three indole derivative probes *N*-2-(3-indolyl)ethyl-tetradecanoyl carboxamide (*N*-myrTAM), 2-tetradecanoyl carboxamidyl-3-(3-indolyl)propanoic acid (*N*-myrTRP) and 11-*N*(2-[3-indolyl]ethylamino)-9-en-methyloxy carbonyldecenate (11-TAMundec) were studied in solvents of different polarities in pure lysophosphatidylcholine micelles (lysoPC) and in total brain gangliosides (TBG) micelles using steady-state and phase-modulation fluorometry. By comparing the fluorescence emission spectra in solvent mixtures with the spectra in lipid micelles it is concluded that the probes detect a more polar environment in TBG compared to lysoPC micelles. Quenching experiments with acrylamide indicate that the indole group of *N*-myrTRP and *N*-myrTAM are more exposed to the aqueous medium than the indole group of 11-TAMundec both in lysoPC and TBG micelles. Quenching of the indole fluorescence with brominated fatty acid at the position 9-10 of the acyl chain is in the following order: 11-TAMundec > *N*-MyrTAM > *N*-MyrTRP in lysoPC micelles whereas in TBG micelles only 11-TAMundec fluorescence is quenched. Based on the results of accessibility of the probes to the aqueous quencher and the dielectric constant calculated for their environment, we estimated the surface to core polarity gradient of the micelles. The polarity gradient is higher in TBG micelles compared to lysoPC micelles.

Keywords: Polarity gradient; Gangliosides; Monolayer; Tryptophan fluorescence; Solvatochromic probe

Abbreviations: *N*-myrTAM *N*-2-(3-indolyl)ethyl-tetradecanoyl carboxamide; *N*-myrTRP, 2-tetradecanoyl carboxamidyl-3-(3-indolyl)propanoic acid; 11-TAMundec, 11-*N*(2-[3-indolyl]ethylamino)-9-en-methyloxy carbonyldecenate; lysoPC L- α -lysophosphatidylcholine; TBG, total brain gangliosides (21% G_{M1}, 42% G_{D1a}, 18% G_{D1b} and 19% G_{T1b}); G_{M1}, Gal β 1 \rightarrow 3Gal-NAc β 1 \rightarrow 4Gal(3 \leftarrow 2xNeuAc) β 1 \rightarrow 4Glc β 1 \rightarrow Cer; G_{D1a}, NeuAc α 2 \rightarrow 3Gal β 1 \rightarrow 3Gal-NAc β 1 \rightarrow 4Gal(3 \leftarrow 2xNeuAc) β 1 \rightarrow 4Glc β 1 \rightarrow Cer; G_{D1b}, Gal β 1 \rightarrow 3Gal-NAc β 1 \rightarrow 4Gal(3 \leftarrow 2xNeuAc8 \leftarrow 2xNeuAc) β 1 /tr 4Glc β 1 \rightarrow Cer; G_{T1b}, NeuAc α 2 \rightarrow 3Gal β 1 \rightarrow 3Gal-NAc β 1 \rightarrow 4Gal(3 \leftarrow 2xNeuAc8 \leftarrow 2xNeuAc) β 1 \rightarrow 4Glc β 1 \rightarrow \pm Cer.

* Corresponding author, Tel.: 54 51 60 8813; Direct laboratory Fax: 54 51 68 0833, Alternative Fax: 54 51 69 4724.

1. Introduction

Gangliosides are complex anionic glycosphingolipids. The negative charge is due to the presence of one or more sialic acids at the polar head group. Gangliosides are mainly localized at the cell surface and they have been postulated to be involved in several membrane-mediated processes of information transduction [1, 2].

Gangliosides affect several physicochemical and structural properties of membranes such as curvature radius, lateral organization, thermotropic behavior and electrostatic interactions [3–5]. The surface potential of ganglioside-containing bilayers has a maximum that is displaced by 1–2 nm from the interface due to the position of the negative charge of the sialic acids along the oligosaccharide chain protruding into the aqueous phase [6–8]. It is also expected that the extensive hydration of the carbohydrate polar head group [9] influences the dielectrical properties of the interface.

The basic amphiphilic peptide melittin and myelin basic protein preferentially interact with gangliosides compared to negative phospholipids in monolayers at the air-water interface [10]. The lipid-peptide interaction takes place with an increase of the surface stability of both the lipid and the peptide, it is thermodynamically favorable, and occurs with dehydration of the glycosphingolipids polar head group [11]. These complex glycolipids also meet the condition of high local surface charge density for a favorable interaction with the ACTH hormone [12]. Using the solvatochromic probe PRODAN a decrease was observed in the interfacial polarity at the adhesive junction between two model membranes containing ganglioside compared to pure phospholipid [13].

In a previous study of the micropolarity of lipid interfaces containing phospholipids mixed with gangliosides, the solvatochromic dye MC-540 [14] and the solvent polarity indicator ANS were used [15]. These reports provided the first indications that the polarity of the head group region of ganglioside-containing interfaces is higher than in pure neutral phospholipids. Nevertheless, it cannot be completely ruled out that the changes in the spectra of these probes induced by the incorporation of gangliosides into the lipid aggregate [14, 15]

may be due to changes in the location of ANS and MC-540. ANS for example, does not bind to pure gangliosides micelles (Bagatolli and Fidelio, unpublished results).

In the present work we have addressed the study of the polarity of interfaces containing gangliosides by using three indole-containing fluorescent probes (Fig. 1). These hydrophobic probes have the advantage that the location of the fluorophor within the lipid aggregate can be determined with more certainty. We have attached a myristic acid to the amine group of tryptophan and tryptamine *N*-myrTRP and *N*-myrTAM; these two molecules, one negatively charged and one neutral, are intended to probe the polar head group environment and the interfacial region close to the surface. A third indole derivative, 11-TAMundec, was made by attaching the tryptamine to the C₁₁ of the undecylenic acid methyl ester in order to sense the properties of the hydrocarbon region of lipid bilayers or micelles. Information from quenching experiments with the soluble acrylamide quencher and with a hydrophobic brominated fatty acid quencher help to set the position of the fluorophor in the micelle in a more predictable manner. We have chosen the indole group because its spectro-

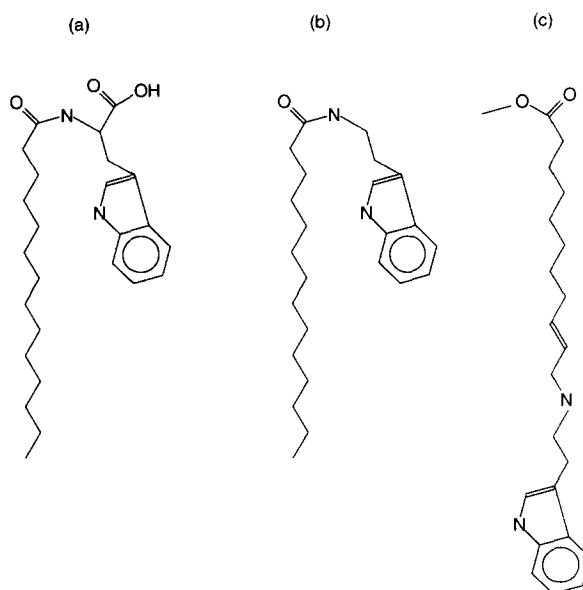


Fig. 1. Formulae of (a), *N*-myrTRP; (b), *N*-myrTAM; and (c), 11-TAMundec.

scopic properties are sensitive to the dielectric constant of the microenvironment [16]. Besides, substituted indoles are particularly useful for mimicking the photophysics of proteins in amphipathic medium [17] which will be used with advantage for future work.

2. Materials and methods

2.1. Materials

Ninhydrin test reagent was from Dupont. Myristic acid was purchased from Eastman Organic Chemistry and was recrystallized from methanol solution before synthesis. L-tryptophan, L-tryptamine, L- α -lysophosphatidylcholine from egg yolk, acrylamide, oleic acid methyl ester, undecylenic acid methyl ester and thionyl chloride were purchased from Sigma Chemical Co. (St Louis, MO). Brominated fatty acid: 9,10-dibromooctadecanoic acid was prepared in our laboratory by alkene bromination of oleic acid methyl ester with subsequent ester hydrolysis and further purification on a silicic acid column. G_{M1} was obtained as described previously [18] and total bovine brain gangliosides (TBG, 21% G_{M1} , 42% G_{D1a} , 18% G_{D1b} , and 19% G_{T1b}) were a gift from Laboratorios Beta, Buenos Aires, Argentina. The solvents used for probes synthesis were purchased from Merck (Córdoba, Argentina) and were dried after distillation with sodium thread. The solvents used in the fluorescence experiments (spectroscopic grade) were obtained from Sintorgan (Buenos Aires, Argentina).

2.2. Synthesis of the probes

N-myrTRP and *N*-myrTAM were prepared by reaction of tryptamine and tryptophan with myristoyl chloride.

Myristoyl chloride. Thionyl chloride was added dropwise to a stirred and cooled solution of myristic acid in CH_2Cl_2 . The product was purified by distillation under reduced pressure. IR (KBr) $_{\nu_{max}}$ 2920, 2850, 1800, 1468, 1405, 980, 955, 725 cm^{-1} . 1H -NMR ($CDCl_3$) δ 0.8–0.9 (t, 3H), 1.2–1.6 (m, 22H), 2.9 (t, 2H).

N-myrTAM. A solution of myristoyl chloride in CH_2Cl_2 was added to a cool and stirred mixture of tryptamine and K_2CO_3 in CH_2Cl_2 . The reaction

mixture was heated under reflux for 20 h, allowed to cool at room temperature and filtered. The organic layer was washed three times with water and dried with $MgSO_4$; the solvent was removed and the residue was purified by silica column chromatography. The elution solvent was chloroform/methanol (24:1, v/v). The product was negative to the ninhydrin reaction. TLC R_f = 0.82 run in chloroform/methanol (24:1, v/v). Melting point = 104–105°C. IR (KBr) $_{\nu_{max}}$ 3401, 3249, 3085, 2933, 2841, 1653, 1637, 1571, 1466, 1097, 744 cm^{-1} . 1H -NMR ($CDCl_3$) δ 0.8–0.9 (t, 3H), 1.2–1.6 (m, 22H), 2.1–2.2 (t, 2H), 3.0 (t, 2H), 3.6 (t, 2H), 5.7 (bs, 1H), 7.0–7.6 (m, 4H $_{Ar}$, 1H CH indol), 8.1 (bs, 1H NH indol). The extinction coefficient is 54 294 $M^{-1} cm^{-1}$ in ethanol at 280 nm.

N-MyrTRP. A suspension of tryptophan and K_2CO_3 in dry dimethylformamide was added dropwise to a solution of myristoyl chloride in CH_2Cl_2 . The mixture was stirred at 80°C for 4 h. The reaction mixture was concentrated and treated with 20 ml of CH_2Cl_2 . After removing the precipitate, the filtrate was washed with water dried with $MgSO_4$ and the solvent evaporated. The residue was chromatographed on silica column. The elution solvent was chloroform/methanol (9:1, v/v). The eluate was evaporated under reduced pressure. The product was negative to the ninhydrin reaction. TLC R_f = 0.35 run in chloroform/methanol (9:1, v/v). Melting point = 150–152°C. IR (KBr) $_{\nu_{max}}$ 3840, 3401, 3361, 2927, 2854, 1727, 1649, 1558, 1445, 1240, 1211, 738 cm^{-1} . 1H -NMR ($CDCl_3$) δ 0.8–0.9 (t, 3H), 1.2–1.6 (m, 22H) 2.1–2.2 (t, 2H), 3.4 (d, 2H), 4.9 (t, 1H), 6.1 (bs, 1H), 7.0–7.6 (m, 4H $_{Ar}$, 1H CH indole) 8.3 (bs, 1H NH indole). The extinction coefficient is 53 497 $M^{-1} cm^{-1}$ in ethanol at 280 nm.

11-TAMundec. The synthesis was made in two steps. *N*-Br succinimide was added to a solution of undecylenic acid methyl ester in Cl_4C . The reaction mixture was exposed to continuous UV radiation for 4 h. The 9-Br-10-undecenoic acid methyl ester reaction product was added to a suspension of tryptamine and K_2CO_3 in dimethylsulfoxide. The mixture was stirred at 25°C for 5 h, obtaining two products: 9-tryptamine-10-undecenoic acid methyl ester and 11-tryptamine-9-undecenoic acid methyl ester with a reaction yield of 20% and 80%.

respectively. The products were chromatographed on silica column. The elution solvent was chloroform/benzene/methanol (15:5:2, v/v). TLC $R_f = 0.88$ run in chloroform/methanol (24:1 v/v). IR (KBr) ν_{\max} 3374, 3286, 2933, 2854, 1740, 1675, 1621, 1461, 1443, 1231, 746 cm^{-1} . $^1\text{H-NMR}$ (CDCl_3) δ 1.3 (m, 8H), 1.6 (m, 2H) 2.0 (q, 2H), 2.3 (t, 2H), 3 (t, 2H), 3.55 (t, 2H), 3.65 (s, 3H) 3.8 (d, 2H), 5.5 (m, 2H), 7–7.6 (m, 4H_{Ar}, 1H CH indole), 8.0, (bs 1H NH indole). The extinction coefficient is 54 325 $\text{M}^{-1} \text{cm}^{-1}$ in ethanol at 280 nm. The product was negative to the ninhydrin reaction.

2.3. Methods

Stock solutions of all probes and lysoPC were stored in chloroform/methanol (2:1, v/v) and in chloroform/methanol/NaOH 20 mM (60:30:4.5, v/v) for TBG and G_{M1} gangliosides. Samples were prepared by mixing lipid and probe (100:1, molar ratio) from the stock solutions and removing the solvent with a stream of N₂. Then the sample was left under vacuum overnight. The dry lipid/probe mixtures were hydrated in buffer Tris–HCl 20 mM/NaCl 50 mM pH 7.4 for 2 h at 60°C, and vortexed. The final probe concentration in the samples was 1 or 3 μM as indicated in the legends of the figures. According to the lipid/probe molar ratio used in all the experiments we assume a random distribution of the probe in the micelle.

Corrected fluorescence steady-state spectra were recorded with a SLM-Aminco Spectrofluorimeter model 4800 C with thermostated cell holder equipped with a magnetic stirrer. Fluorescence intensity was corrected by inner filter effects [19] and dilution. All the fluorescence experiments were done in quadruplicate at 25°C. The λ_{\max} from the emission spectra was determined by the first derivative using the original software from SLM. The excitation wavelength was 295 nm in all fluorescence experiments. The fluorescence phase-shift and modulation lifetime determinations were measured at 30 and 18 MHz. The fluorescence was observed using a cut-off filter (310 nm) to eliminate scattering radiation from the light source. In the reference cell a solution of *p*-terphenyl in ethanol was used to correct possible color effects [20]. Data analyses were made according to the software package of the SLM 4800C. Data were

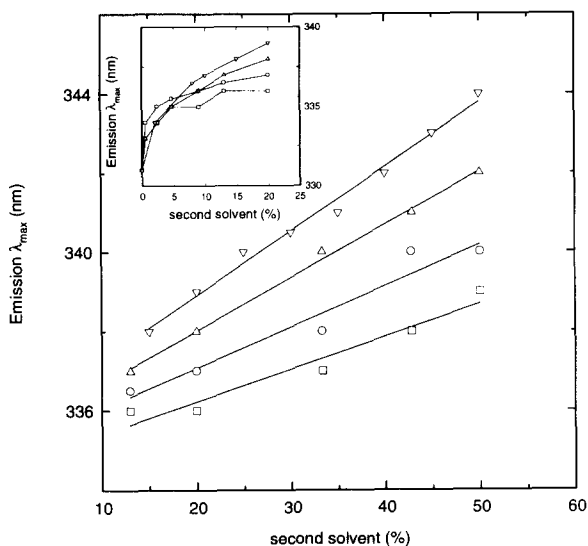


Fig. 2. Variation of λ_{\max} of the fluorescence emission spectra of *N*-myrTRP in mixtures of dioxan with a protic or non-protic second solvent: acetonitrile (\square), methanol (\triangle), dimethylformamide (\circ), water (∇). The insert shows the non-linear relation between λ_{\max} and the proportion of the second solvent between 0% and 10% where the specific solvent effect is observed (see text).

collected until the standard deviation from each measurement of phase and modulation were at most 0.2 and 0.004, respectively. The dielectric constant of the solvents mixtures were obtained as described previously [21].

3. Results

3.1. Fluorescence properties of *N*-myrTRP, *N*-myrTAM and 11-TAMundec in organic solvent solution

The fluorescence of the indole group of *N*-myrTRP, *N*-myrTAM and 11-TAMundec is sensitive to the polarity of the medium. The fluorescence emission maximum (λ_{\max}) shifts to the red region of the spectra when the dielectric constant of the solvent increases. Fig. 2 shows the dependence of λ_{\max} of *N*-myrTRP in binary mixtures of dioxan with a protic solvent, methanol and water, or with a non-protic solvent, dimethylformamide and acetonitrile. It can be observed that the increase in λ_{\max} with the dielectric constant is steeper at lower proportions of the second solvent ($< 10\%$). Similar results were obtained for

N-myrTAM and 11-TAMundec. The small changes in the dielectric constant due to the presence of the second solvent in the range of 0–10% are not responsible for the steep increment in λ_{\max} . In this range the changes are mainly due to specific solvent effect [22]. At proportions of the second solvent above 10% the specific solvent effect saturates and the changes in λ_{\max} are due to changes in the solvent dielectric constant. We have used the range where λ_{\max} increases linearly with the dielectric constant (above 10% v/v of water in dioxan) to obtain a correlation curves of λ_{\max} vs. dielectric constant for the three probes. These relations were used to estimate the polarity of the microenvironment of the different probes in lysoPC and TBG micelles. Fig. 3 shows the dependence of the emission maximum for *N*-myrTRP and *N*-myrTAM in dioxan/water mixtures as a function of the dielectric constant. In the case of *N*-myrTAM, the curve was made up to a dielectric constant ϵ of 42 due to the formation of probe aggregates at higher water proportions. The functional relationship between λ_{\max} and ϵ is described by the following equations fitted by linear regression:

$$\epsilon = \lambda_{\max} 4.03 - 1.355 \quad (1)$$

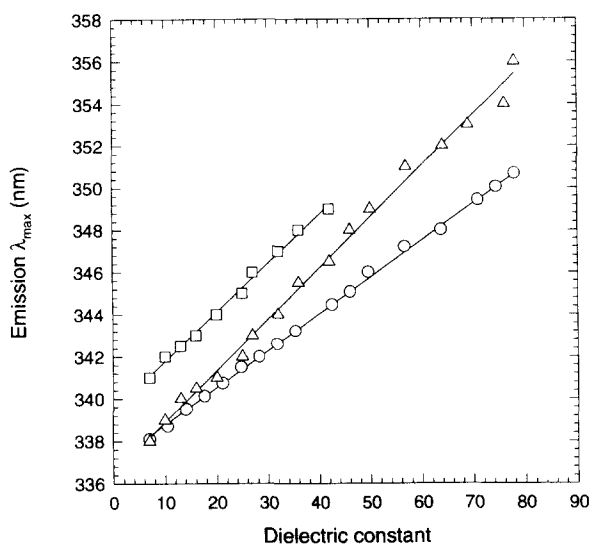


Fig. 3. The variation of λ_{\max} of the fluorescence emission spectra of *N*-myrTAM (\square), *N*-myrTRP (Δ) and 11-TAMundec (\circ) with the dielectric constant, ϵ , in mixtures of dioxan/water. The probe concentration was 1 μ M.

$$\epsilon = \lambda_{\max} 4.31 - 1.463 \quad (2)$$

$$\epsilon = \lambda_{\max} 5.72 - 1.929 \quad (3)$$

Eqs. 1, 2 and 3 were for *N*-myrTRP, *N*-myrTAM and 11-TAMundec, respectively.

3.2. Fluorescence properties of *N*-myrTRP, *N*-myrTAM and 11-TAMundec in lysoPC and ganglioside micelles

For all probes we have measured the position of the emission peak, the fluorescence quenching by the soluble quencher acrylamide and the fluorescence quenching by a brominated fatty acid in micelles of lysoPC and TBG. These measurements provide information about the location of the indole group and its micropolarity in different regions of the micelle. These probes are strongly hydrophobic and the partitioning from the micelle into the aqueous medium is practically null, leading to a negligible contribution to the fluorescence signal from probe in the bulk water. In this connection, using the lipid monolayers technique, we have found that all probes form stable insoluble isotherms with molecular areas within 0.55–0.60 nm²/molecule at 15 mN·m⁻¹ (data not shown).

The fluorescence emission from each indole derivative in TBG was red-shifted compared to lysoPC micelles. The shift in λ_{\max} was independent on the lipid/probe molar ratio greater than 10:1. This indicates that the probe detects a more polar environment in TBG or G_{M1} compared to lysoPC micelles (Table 1). The positions of the emission peak are summarized in Table 1. Inserting the values of λ_{\max} in Eqs. 1–3, we calculated the dielectric constant of the microenvironment of the chromophores in lysoPC and TBG micelles (see Table 1).

Comparing the results within the same type of micelle it can be seen that the negatively charged *N*-myrTRP detects a more polar environment than the neutral *N*-myrTAM. On the other hand 11-TAMundec, with the indole group attached at position 11 of the hydrocarbon chain, detects the less polar environment. All the probes have the same emission maximum if the ionic strength of the buffer is increased to 0.25 M NaCl.

Table 1

Fluorescence emission maximum of *N*-myrTRP, *N*-myrTAM and 11-TAMundec and the dielectric constant detected in lysoPC and gangliosides micelles

Mixture (lipid/probe) ^a	λ_{\max} (nm)	ϵ
lysoPC/ <i>N</i> -myrTRP	345	35
lysoPC/ <i>N</i> -myrTAM	344	20
lysoPC/11-TAMundec	340	17
G_{M1} / <i>N</i> -myrTRP	347	43
G_{M1} / <i>N</i> -myrTAM	347	33
G_{M1} /11-TAMundec	341	21
TBG/ <i>N</i> -myrTRP	348	47
TBG/ <i>N</i> -myrTAM	347	33
TBG/11-TAMundec	342	22

^aLipid/probe ratio 100:1.

The exposure of the indole group to the aqueous medium was evaluated by quenching the fluorescence emission of the probes by acrylamide (Fig. 4 and Table 2). We used a modified form of

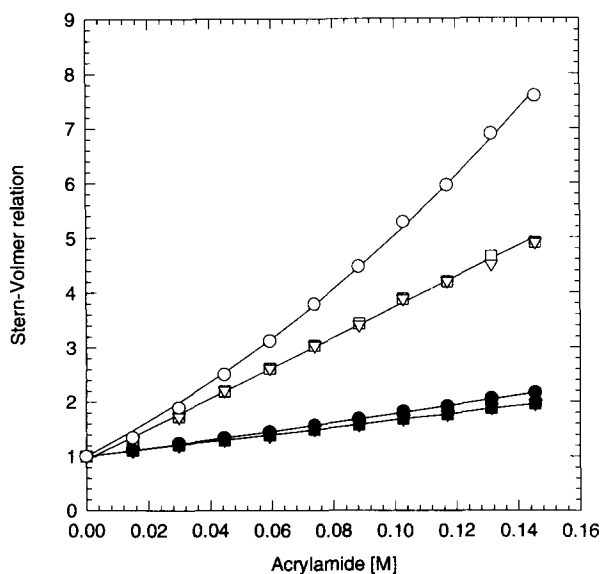


Fig. 4. Stern-Volmer plots for the quenching with acrylamide of the fluorescence from *N*-myrTRP in Tris-HCl 20 mM/NaCl 50 mM pH 7.4 (open symbols) and in TBG micelles (closed symbols). The lipid/probe molar ratio was 100:1. The total probe concentration was 3 μ M. The Stern-Volmer relations are as follows: F_0/F , (○); τ_0/τ , (▽); and $F_0/F_{e^{1Q}}$, (◻).

the Stern-Volmer equation which allows to evaluate the contribution from the static quenching [23]:

$$F_0/F = e^{VQ}(1 + K_{SV}[Q]) \quad (4)$$

where F and F_0 are the fluorescence intensities in the presence and in the absence of quencher Q , respectively; K_{SV} is the Stern-Volmer constant defined as

$$K_{SV} = \tau_0 k_q$$

where τ_0 is the fluorescence lifetime in the absence of quencher k_q is the collisional rate constant for the quenching process; V is the static quenching constant [23]. K_{SV} and V were obtained from the best fit of the experimental data to Eq. 4. The k_q values were calculated using the experimental τ_0 values shown in Table 2. The rate constant k_q (for the collisional component of quenching) is a kinetic measure of the exposure of the indole group to the aqueous medium [23, 24]. A general trend can be extracted from the values shown in Table 2. Higher values of k_q were obtained for the quenching of the indole group of each probe when inserted into lysoPC compared to TBG micelles. Also, slightly higher values of k_q were found for *N*-myrTRP compared to *N*-myrTAM whatever the type of the lipid-forming micelle. These results indicate that *N*-myrTRP is a little more accessible than *N*-myrTAM. As expected, even lower values of k_q were observed for 11-TAMundec in lysoPC and TBG micelles indicating a smaller accessibility of the indole group to the aqueous medium (see Table 2). Additional information on the chromophore accessibility can be obtained from the value of the static quenching constant V . This parameter measures the probability of finding a quencher molecule next to the indole group in the ground-state level [23]. It should be noticed that larger values of V for *N*-myrTAM and *N*-myrTRP were obtained in TBG than in lysoPC (see Table 2). Negligible values of V , which indicates absence of static quenching, were obtained for the indole group in the 11-TAMundec probe. Fig. 4 shows the classical Stern-Volmer plot (F_0/F vs. concentration of quencher) for *N*-myrTRP

Table 2

Quenching parameters for the interaction of the indole group of *N*-myrTRP, *N*-myrTAM and 11-TAMundec in lysoPC and gangliosides micelles with the soluble acrylamide quencher

Mixture (lipid/probe) ^a	K_{sv} (M ⁻¹)	V (M ⁻¹)	τ_o (ns)	$k_q \times 10^{-9}$ (M ⁻¹ .s ⁻¹)
lysoPC/ <i>N</i> -myrTRP	7.42	0.108	6.54	1.135
lysoPC/ <i>N</i> -myrTAM	7.49	0.409	7.38	1.015
lysoPC/11-TAMundec	4.33	~0	6.58	0.660
TBG/ <i>N</i> -myrTRP	6.58	0.690	6.65	0.989
TBG/ <i>N</i> -myrTAM	5.87	0.979	6.69	0.878
TBG/11-TAMundec	4.40	~0	7.10	0.620
<i>N</i> -myrTRP ^b	27.33	2.992	5.10	5.359

^aLipid/probe ratio 100:1.

^bBelow its critical micelle concentration (CMC).

below its CMC and inserted into TBG micelles. This figure also shows the modified Stern-Volmer plot ($F_o/F_e^{[Q]}$) and the dynamic relation (τ_o/τ , where τ is the fluorescence lifetime in presence of quencher) vs. concentration of quencher. Upwards bending in the classical Stern-Volmer plots is observed for the quenching of pure *N*-myrTRP at a concentration below the critical micellar concentration or inserted into TBG micelles (see Fig. 4). Similar behavior was found for *N*-myrTRP in lysoPC micelles and *N*-myrTAM in lysoPC and TBG micelles (data not shown).

A plot of τ_o/τ vs. quencher concentration reflects the dynamic contribution to the quenching and it is described by the classical Stern-Volmer equation which does not include the factor $\exp(V/[Q])$ (see ref. [23]). The values for V calculated by fitting the experimental results to Eq. 4 are shown in Table 2. The calculated values of $F_o/F_e^{[Q]}$ were plotted vs. quencher concentration (Fig. 4). The linear plot obtained in this way agrees with the experimental relation of τ_o/τ vs. quencher concentration. Taken these findings together, it can be concluded that K_{sv} and V values shown in Table 2 represent correctly both the dynamic and static contribution to the quenching process.

Further assessment for the location of the probes was obtained by quenching the fluorescence with a fatty acid dibrominated at position 9 and 10 of the acyl chain. Bromides are located in the hydrophobic core of the micelles and a

fluorophor localized at this region will be more quenched than those located near to the polar head group/water interface. Bromolipids were previously defined as short range quenchers and quenching becomes significant only when the tryptophan and bromides are very close [25]. It has been demonstrated that bromolipids are capable of determining the position of a tryptophan in a membrane [25, 26]. A distance of 10–12 Å of the bromides from the head group/hydrocarbon interface can be estimated for the case that the bromides are localized at position 9–10 of the fatty acid acyl chain [26]. As expected the indole of 11-TAMundec is more quenched than *N*-myrTRP and *N*-myrTAM that have the indole group more exposed to the aqueous medium (Table 3). The extent of the quenching of 11-

Table 3

Interaction of the indole group of *N*-myrTRP, *N*-myrTAM and 11-TAMundec in lysoPC and gangliosides micelles with the hydrophobic brominated fatty acid quencher

Mixture (lipid/probe) ^a	% of quenching
lysoPC/ <i>N</i> -myrTRP	2
lysoPC/ <i>N</i> -myrTAM	8.2
lysoPC/11-TAMundec	20.5
TBG/ <i>N</i> -myrTRP	0
TBG/ <i>N</i> -myrTAM	0
TBG/11-TAMundec	17

^aLipid/probe/quencher ratio 100:1:20.

TAMundec is similar either in lysoPC or TBG micelles (see Table 3). Quenching of *N*-myrTRP or *N*-myrTAM with the brominated fatty acid did not occur in TBG micelles. For lysoPC micelles, the quenching of *N*-myrTRP caused by the brominated fatty acid was almost negligible whereas the extent of quenching reaches 8% for *N*-myrTAM (about 40% less quenchable than the hydrophobic 11-TAMundec, Table 3).

4. Discussion

The probes we have synthesized with the indol group attached at different region of a fatty acid are intended to give a more rational information about the localization and the environment that they are sensing (Fig. 1). Comparison of the position of the emission peak with those observed in solvent mixtures of different dielectric constant indicates that the microenvironment sensed by all probes in the gangliosides micelles is more polar than in lysoPC micelles.

The negatively charged *N*-MyrTRP detects a more polar microenvironment than the neutral *N*-MyrTAM. *N*-MyrTAM senses a dielectric constant of 33 in TBG micelles, about 14 units lower than the value of $\epsilon = 47$ measured with *N*-MyrTRP (Table 1). These values are similar to those measured at the surface of micelles for several detergents [27]. The range of the dielectric constant observed in lysoPC micelles is similar to the value measured with MC-540 in egg phosphatidylcholine vesicles [28] and the same difference of about 14–15 dielectric constant units between both probes was measured in lysoPC micelles (Table 1).

The higher polarity observed in TBG can be due to a real difference in the micropolarity or to a different location of the probes. Quenching of the fluorescence with the water-soluble, electrically neutral quencher acrylamide indicates that *N*-myrTRP and *N*-myrTAM are slightly more accessible to the aqueous medium in lysoPC compared to TBG micelles (see the k_q values in Table 2). In spite of the lower accessibility, the polarity of the microenvironment detected by all probes in ganglioside micelles are higher. This suggests that the more polar environment detected by these

probes in TBG is mainly due to the intrinsic differences between both type of interfaces. Within the same type of micelles, slightly larger values of k_q are observed for *N*-myrTRP compared to *N*-myrTAM. It is reasonable to expect that the negative charge at the polar head group of *N*-myrTRP probe requires to be located closer to the aqueous medium. The higher values of static quenching constant V together with lower values of dynamic constant k_q found for *N*-myrTRP and *N*-myrTAM in ganglioside micelles compared to lysoPC aggregates (Table 2) indicates a higher concentration of the quencher with a restriction for diffusion at the ganglioside head group region.

On the other hand, the indole in 11-TAMundec is clearly less exposed than the other probes either in lysoPC or TBG micelles. According to the k_q and V values (Table 2) and the extent of quenching by the brominated fatty acid (Table 3, see below) it can be deduced that the location of the indole group in 11-TAMundec probe is the same in both kind of micelles. Because the location is similar, the differences detected in the fluorescence emission spectra (Table 1) indicate that the inner core in TBG is more polar than in lysoPC micelles. This may be because the large and hydrated polar head group of gangliosides produces a higher gradient of polarity towards the hydrophobic core.

Quenching of the fluorescence with the 9-10 brominated fatty acid in lysoPC micelles indicates that the indole group in the *N*-myrTRP is more distant from the inner core than the indole group in the *N*-myrTAM. Because more quenching is observed, we can conclude that 11-TAMundec sets its indole group deeper in the micelle (Table 3). The location of the probes according to this criteria is in complete agreement with the results from the acrylamide quenching experiments (Table 2, see above). If we correlate the location of the indoles with the polarity estimated we can conclude that a gradient of polarity is observed. Taking into account all the results, we suggest that the indole group in *N*-myrTRP probe which is closer to the aqueous medium detects the environment near the polar head group; the indole in *N*-myrTAM which is little more buried detects the

environment of the interfacial region corresponding to the glycerol backbone and the buried indole in 11-TAMundec detects the hydrocarbon core region. Even though we have not precisely determined independently the position of the bromide atoms in the micelles, it is clear that the distance between the bromides and the indole of *N*-myrTRP and 11-TAMundec in TBG is larger than in the lysoPC micelles because no quenching is observed (Table 3).

The present work expands our previous studies on the micropolarity of interfaces containing gangliosides [14, 15]. Even if slight differences in the location of the probes contributes to the differences in the emission spectra of probes in lysoPC compared to the ganglioside micelles, our results strongly suggest that the inner core and the polar head group region of ganglioside-containing micelles are more polar than the corresponding regions of lysoPC micelles.

The consensus dielectric constant gradient in a bilayer was about 70 from the membrane aqueous surface to 5 at the bilayer center [29]. Using the indole-derivative probes we have found that there is dielectric constant gradient between the polar head group region to the inner core ranging from 35 to 17 and from 47 to 22 for LysoPC and gangliosides micelles, respectively (Table 1). The values found for the hydrophobic core is in agreement with the higher value expected for a more hydrated center of the micelle compared to the more rigid packed bilayer. The steepness of the gradient in an amphiphile lipidic structure will depend on the degree of hydration and the water penetrating capability given by the type of the lipid, head group, physical state and topological properties of the lipid organization.

Acknowledgements

This work was supported in part by grants from CONICOR SeCyT-UNC, Fundación Antorchas and CONICET. GDF and JDP are members of the CONICET Investigator Career and LAB is a CONICET Fellow, Argentina. The authors are grateful to Prof. Dr. B. Maggio for critical reading of the manuscript.

References

- [1] G. Tettamanti (1988) Towards the understanding of the physiological role of gangliosides, in: R.W. Ledeen, E.L. Hogan G. Tettamanti, A.J. Yates and R.K. Yu (Eds.), *New Trends in Gangliosides Research: Neurochemical and Neuroregenerative Aspect Fidia Research Series*, Liviana Press, Padova, pp. 625–646.
- [2] R.K. Yu and M. Saito (1989) Structure and localization of gangliosides, in: R.U. Margolis and R.K. Margolis (Eds.) *Neurobiology of Glycoconjugates* Plenum Publishing Corporation, New York, pp. 1–42.
- [3] B. Maggio (1985) Geometric and thermodynamic restrictions for the self-assembly of glycosphingolipids-phospholipids systems. *Biochim. Biophys. Acta* 815, 245–250.
- [4] B. Maggio, G.G. Montich and F.A. Cumar (1988) Surface topography of sulfatide and gangliosides in unilamellar vesicles of dipalmitoylphosphatidylcholine. *Chem. Phys. Lipids* 46 137–146.
- [5] B. Maggio, (1994) The surface behaviour of glycosphingolipids in biomembranes: A new frontier of molecular ecology. *Prog. Biophys. Mol. Biol.* 62, 55–117.
- [6] B. Maggio, F.A. Cumar and R. Caputto (1978) Surface behavior of gangliosides and related glycosphingolipids. *Biochem. J.* 171, 559–565.
- [7] B. Maggio, F.A. Cumar and R. Caputto (1978) Configuration and interactions of the polar head group in gangliosides. *Biochem. J.* 189, 435–440.
- [8] A.P. Winiski, M. Eisemberg, M. Langner and S. McLaughlin (1988) Fluorescent probes of electrostatic potential 1 nm from the membrane surface. *Biochemistry* 27, 386–392.
- [9] D. Bach, B. Sella and I.R. Miller (1982) Compositional aspects of lipid hydration. *Chem. Phys. Lipids* 31, 381–394.
- [10] G.D. Fidelio, B. Maggio and F.A. Cumar (1982) Interaction of soluble and membrane proteins with monolayers of glycosphingolipids. *Biochem. J.* 203, 717–725.
- [11] G.D. Fidelio, B. Maggio and F.A. Cumar (1986) Interaction of melitin with glycosphingolipids and phospholipids in mixed monolayers at different temperatures. Effect of the lipid physical state. *Biochim. Biophys. Acta* 862, 49–56.
- [12] P.F.J. Verhallen, R.A. Demel, H. Zwiers and W.H. Gispen (1984) Adrenocortic hormone (ACTH)-lipid interactions. Implications for involvement of amphipatic helix formation. *Biochim. Biophys. Acta* 775, 246–254.
- [13] G.J. Brewer (1992) Polarity decrease at the adhesive junction between two model membranes containing gangliosides. *Biochemistry* 31, 1809–1815.
- [14] G.G. Montich, M.M. Bustos, B. Maggio and F.A. Cumar (1985) Micropolarity of interfaces containing anionic and neutral glycosphingolipids as sensed by merocyanine-540. *Chem. Phys. Lipids* 38, 319–326.
- [15] G.G. Montich, J.A. Cosa and B. Maggio (1988) Interaction of 1-anilino-naphthalene 8-sulfonic acid with interfaces containing cerebrosides, sulfatides and gangliosides. *Chem. Phys. Lipids* 49, 111–117.

- [16] D. Creed (1984) The photophysics and photochemistry of the near-UV absorbing amino acids. I. Tryptophan and its simple derivatives. *Photochem. Photobiol.* 39, 537–562.
- [17] Y. Chen, F. Gai and J.W. Petrich (1994) Single-exponential decay of the nonnatural amino acid 7-azatryptophan and the nonexponential fluorescence decay of tryptophan in water. *J. Phys. Chem.* 98, 2203–2209.
- [18] G.D. Fidelio, T. Ariga and B. Maggio (1991) Molecular parameters of gangliosides in monolayers. Comparative evaluation of suitable purification procedures. *J. Biochem.* 110, 12–16.
- [19] J.R. Lakowicz (Ed.) (1983) Instrumentation for fluorescence spectroscopy, in *Principles of Fluorescence Spectroscopy*, Plenum Press, New York pp. 49–47.
- [20] J.R. Lakowicz (Ed.) (1983) Measurement of fluorescence lifetimes, in *Principles of Fluorescence Spectroscopy*, Plenum Press, New York pp. 87–89.
- [21] J. Bramhall (1986) Phospholipid packing asymmetry in curved membranes detected by fluorescence spectroscopy. *Biochemistry* 25, 3479–3486.
- [22] J.R. Lakowicz (Ed.) (1983) Effects of solvents on fluorescence emission spectra, in *Principles of Fluorescence Spectroscopy*, Plenum Press, New York, pp. 201–205.
- [23] M.R. Eftink and A. Ghiron (1976) Fluorescence quenching of indole and model micelle systems. *J. Phys. Chem.* 80 486–493.
- [24] M.R. Eftink and C.A. Ghiron (1976) Exposure of tryptophanyl residues in proteins. Quantitative determination by fluorescence quenching studies. *Biochemistry* 15, 672–680.
- [25] E.J. Bolen and P.W. Holloway (1990) Quenching of tryptophan fluorescence by brominated phospholipids. *Biochemistry* 29, 9638–9643.
- [26] T.J. McIntosh and P.W. Holloway (1987) Determination of the depth of bromine atoms in bilayers formed from bromolipid probes. *Biochemistry* 26, 1783–1788.
- [27] J.F. Tocanne and J. Teissie (1990) Ionization of phospholipids and phospholipids-supported interfacial lateral diffusion of protons in membrane model systems. *Biochim. Biophys. Acta* 1031, 111–142.
- [28] B. Ehrenberg and E. Peuzner (1992) Spectroscopic properties of the potentiometric probe merocyanine-540 in solutions and liposomes. *Photochem. Photobiol.* 57, 228–234.
- [29] C.D. Stubbs, C. Ho and S.J. Slater (1995) Fluorescent techniques for probing water penetration into lipid bilayers. *J. Fluoresc.* 5, 19–28.